Electrodes: Flat vs Pin-Type Topology in Alkaline Water Electrolysis

MARÍA JOSÉ LAVORANTE[1], MICAELA FRAGUEIRO FRIAS[1], NELSON JESÚS VICHERA MOLA[1], MARCELO BUSTOS[2]
[1]Research and Development Division of Renewable Energy,
Institution of Scientific and Technological Research for Defense,
Juan Bautista de la Salle 4397, Villa Martelli, Buenos Aires Province,
ARGENTINA

[2]Prototyping Department
Institution of Scientific and Technological Research for Defense,
Juan Bautista de la Salle 4397, Villa Martelli, Buenos Aires Province,
ARGENTINA

Abstract: - The energy transition is already underway, and hydrogen plays a crucial role by enabling renewable energy storage without emitting carbon dioxide and other greenhouse gases. Given the intermittency of renewable energy sources, energy storage is essential in this transition. Hydrogen technologies are recognized as promising solutions. One method to produce green hydrogen is through water electrolysis using renewable energy sources, a process identified with significant potential for decarbonization. However, it needs to enhance efficiency, reduce component costs, and consequently, production costs to expand its adoption. Alkaline water electrolysis for hydrogen production is a mature technology with commercially available megawatt (MW) scale installations. To enhance the performance of alkaline electrolyzers, this study focuses on evaluating flat and pin-type electrodes. To analyze their performance, the electrodes were tested at, 20 degrees Celsius, varying electrode distances between them. Tests were conducted in an electrochemical cell, where different operating voltages were applied incrementally, from 0.1 [V] every 30 seconds, across a range of 0 to 2.7 [V]. From the analyzed distances, the highest current densities were obtained at 1.95 [mm] for the pin type and 4.59 [mm] for the flat. Comparing performances at comparable distances, it is observed that the flat electrode generates a higher current density than the pin type. Although the pin-type electrode increases its surface area by approximately 83%, it hinders the detachment of bubbles, causing them to remain on the electrode's surface for a longer time and reducing its performance.

Key-Words: - Electrodes, pin-type, flat-type, alkaline water electrolysis, performance, hydrogen production, bubble detachment.

Received: May 9, 2024. Revised: September 21, 2024. Accepted: October 23, 2024. Published: November 26, 2024.

1 Introduction

The increase in greenhouse gas emissions in the environment has become an important issue for many world leaders, legislators, researchers, and the world population in general, and that is why each of these groups strives, within their ranges of action, to limit the growing impact of climate change on the environment, [1], [2], [3].

According to the report prepared by the International Energy Agency, global carbon dioxide (CO_2) emissions from energy combustion and industrial processes in 2023 reached a new all-time high of 37.4 Gt. This increase represents around 410 Mt CO_2 released into the atmosphere, with respect to the previous year, [4].

The 21st century brought with it, an extensive development of renewable technologies in order to reduce the generation of electricity through fossil fuels. However, even in this century, most countries still depend on fossil fuels for electricity generation, either due to the lack of technologies, resources, or conditions to implement the production through renewable energies, [5].

Added to this fact, it must not be forgotten that renewable energies are essentially intermittent, and this characteristic presents itself as an obstacle, no less, when it comes to a more generalized implementation. Wind and solar power generation can vary on a range of time scales, ranging from near-instantaneous to seasonal, [6]. Therefore, in a predominantly renewable matrix, this type of

generation must be balanced with demand by implementing energy storage systems, [7]. Systems that allow the accumulation of some form of energy, so that at another time, other than when it is generated, it can be used to perform some useful operation, [8]. Electrical energy presents difficulties for its storage. In general, it requires to be converted into another form of energy, [9]. Among the methods that can be used to store energy can be found in chemical, electrochemical, electrical, mechanical, and thermal systems, [10], [11], [12], [13].

Hence, for the increasing energy demand and consumption, requests for mitigation of greenhouse gas emissions, main responsibility of the global warming, population growth, as well as depletion of natural resources it is of great importance to make the most of renewable energy and this, of course, includes its surplus. The surplus that is generated at times of the day when the demand is less than the generation, [14], [15].

To address these challenges, excess power generated through renewables could be stored in batteries, [16], [17]. Their main advantage is their almost instantaneous response time, that they can be flexibly configured, and their relatively low manufacturing time, while their high investment cost and short useful life are the main disadvantages, [18]. Batteries are suitable for short-term generation-demand balancing, specifically in one day [19], meanwhile, another approached would be to convert that surplus into storable chemicals.

One promising approach is the production of fuels from renewable electricity that can then be used for stationary power production or transportation. This idea was called "power-to-x" in Germany in the early 2010s, where x represents the product to be obtained, [20].

These technologies are presented as a viable option to store excess renewable energy, for its subsequent dispatch for final use, in addition to providing a path to decarbonization and to produce "green" fuels and chemical products, [21]. Through these technologies, hydrogen, methane, ammonia, and hydrogen peroxide could be obtained, to name a few. These energy carriers and chemical compounds can provide versatility in storage (addressing imbalances in renewable resources), transportation, and their subsequent conversion to achieve decarbonization of energy infrastructure, [22].

In other words, the adoption of "power to x" technologies and their products will facilitate the integration of renewable energies in other sectors of the economy such as transportation, agriculture, and manufacturing and, in this way, they will contribute to the effective displacement of the requirement for fossil fuels and their negative effects caused by their production and use, on the environment, [23], [24].

Practically, power-to-hydrogen is the backbone of the power-to-x concept, [25]. Hydrogen can be produced from any type of energy source, but given what it has been mentioned, it is much more attractive if it is obtained from renewable sources. The method is the electrolysis of water, where the latter is the raw material of the process.

The storage concept enlaces the energy and gas networks through the transformation of energy into gas through two main steps: the production of hydrogen through water electrolysis (which can be used directly as fuel) and the conversion of hydrogen into chemicals or fuels compatible with the existing infrastructure for transportation or production, [26].

Hydrogen is perceived as a clean fuel, because when it is used in combustion systems or in fuel cells designed for this purpose, it produces only water as a by-product.

In terms of properties, hydrogen has a high energy per unit mass. Its specific energy is 120 [MJ/kg] at 0° Celsius and 1 atmosphere but has a low energy density by volume 0.01 [MJ/L] under the same conditions of temperature and pressure. Unlike conventional fuels, it has a very small and light molecular structure, but it is important to emphasize its high heating value (HHV) of 141.9 [MJ/kg], which is almost three times that of gasoline, [27].

As it was mentioned previously, since the method of obtaining hydrogen through these technologies is electrolysis, it was going to be present.

To fully understand the meaning of this process, it should start with the word itself. The word electrolysis has the suffix ¨lysis¨, of Greek origin, which means division or rupture, and the prefix ¨electro¨, which refers to the flow of electrical current. For this reason, electrolysis is defined as the process in which a compound is divided into its component elements by passing electricity through it. Electrolysis is a non-spontaneous chemical change, since it does not occur on its own, so electrical energy is the force that drives the process, [28].

The electrolysis of water, then, is the breakdown of the water molecule into hydrogen and oxygen by passing electricity through it, [29].

A basic electrolysis cell consists of two electrodes, a separator/diaphragm or membrane, and the electrolyte, [30]. The latter is an essential part of the basic electrolysis cells since it is the means

responsible for transporting the ionic species generated from one electrode to the other. It functions as a selective conductor through which ions pass but electrons do not. Electrodes are the surfaces on which the oxidation and reduction half-reactions take place. The cathode is the electrode at which reduction takes place. The anode is the electrode at which oxidation takes place. The separator or membrane is responsible for physically setting apart the gaseous products obtained in the cathodic and anodic compartments, avoiding contact between electrodes, and preventing cell short circuits. However, the membrane has an additional function, which is to selectively promote the passage of one or more components.

There are several characteristics that have been used to classify the different types of water electrolyzer, such as the states of aggregation and the type of electrolyte, as well as their operating conditions linked to temperature and pressure, [31]. However, the one that is widely accepted is by the type of electrolyte and this classification allows differentiating four technologies: alkaline, polymeric electrolyte membrane, anion exchange membrane, and solid oxide, [32], [33], [34]. In alkaline-type electrolyzers, a highly concentrated potassium hydroxide solution is used as an electrolyte, which is responsible for the transport of hydroxyl anions. For the other types of electrolyzers, a solid electron-insulating electrolyte is used that, in addition to transporting ionic species, physically separates the gases produced. Water electrolysis plants to produce hydrogen have been identified as a key factor in the production cost of X. To be more specific, in addition to the CAPEX of the electrolyzer, the initial investment for the installation of renewable energies must be considered. Although alkaline electrolysis is the most mature electrolysis technology, if the decarbonization of the energy sector is to be achieved, the other should be developed. The polymeric electrolyte membrane because it presents a better response to energy fluctuations than the alkaline one. Solid oxide because it presents a higher efficiency and lower energy demand. Anion exchange membrane water electrolyzers would provide a promising alternative by combining many benefits of alkaline and proton exchange membrane electrolyzers, [35]. The alkaline working environment allows the use of economical bipolar plates and porous transport, as well as electrocatalysts that do not belong to the platinum group. Furthermore, the implementation of an anion exchange membrane could operate at differential pressure, fast dynamic response, low energy losses, and higher current density, [36], [37].

Given that for the implementation of these technologies at the scale needed, low-cost materials are required, and the manufacturing method can be carried out on an industrial scale, in this work the performance of two types of 316L stainless steel electrodes is proposed to be analyzed in an environment like that of an alkaline type electrolyzer. One pair is the material as purchased from the factory and the other has a pin-type topology on its surface that will allow it to increase its active area by approximately 83%.

2 Materials and Methods

2.1 Construction of the Electrode Topology

Onto the surface of a 110 [mm] length x 111 [mm] width x 3 [mm] thickness, 316L stainless steel electrode, a pin-type topology was applied. It consists of straight vertical and horizontal channels, which intersect, with dimensions of 90 [mm] length x 1 [mm] width x 1 [mm] depth. The channels were made by a universal milling machine using a circular shaped high-speed steel saw of 8.0 x 1.0 [mm] in diameter (SINPAR). These channels then give rise to the pins which, with their side walls of 2 [mm] length x 1 [mm] width, increase the active area of the electrode by approximately 83%, compared to the original electrodes without them. Figure 1(a), shows the image obtained by the Leica stereoscopic microscope with a DFC295 camera, using an increase of 0.63x. The irregularities in the base and sides of the channels can be observed, caused by the tool used in their manufacture, as well as the excess material remaining on the edges of the pins, such as protruding edges and excess material that remains attached, increasing the exposed surface area of the electrode. It should be noted that the burr resulting from the manufacturing method has not been considered in the calculation of the percentage of gained active area. The electrodes submitted to the machining process were those named mechanized electrodes with pin-type topology.

To compare the behavior of this type of geometry, a pair of flat electrodes of the same material were evaluated, with dimensions 110 [mm] length x 110 [mm] width x 2.2 [mm] thickness. Figure 1(b), is an image taken with the Leica stereoscopic microscope, using a magnification of 0.63x.

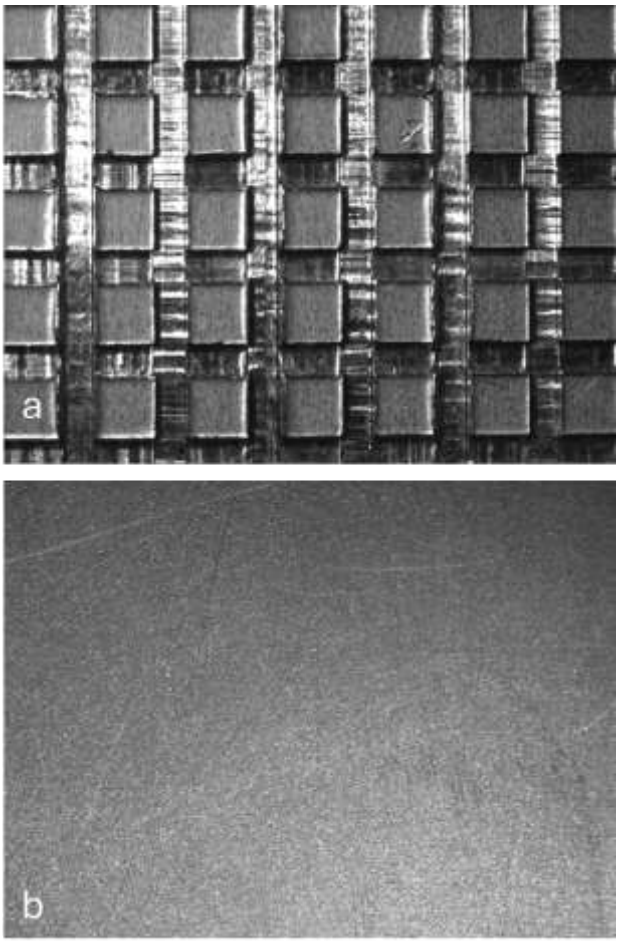

Fig. 1: View of the: a) pin-type topology and b) flat electrodes

2.2 Preparation and Cleaning of the Electrodes

A preparation is undertaken to remove any impurities that may adhere to the surface of the electrodes because of manufacturing and machining processes. Initially, an abrasive product containing sodium dodecyl benzene sulfonate, carbonates, and alkalizing agents is used, followed by thorough rinsing with drinking water. Next washing with a detergent containing anionic surfactants such as sodium lauryl ether sulfate and sodium linear alkylbenzene sulfonate, subsequently by extensive rinsing with drinking water. Finally, two rinses with distilled water are performed.

To ensure that the electrodes are free from any type of impurities before evaluation, the following cleaning treatment is applied to them: a filter paper (one for each electrode) is soaked with acetone (99.5%, Sintorgan), to carefully clean the surface, and allowed solvent to evaporate. Finally, a filter paper (one for each electrode) is soaked with absolute ethyl alcohol (Biopack), which is used to cleanse the surface of the electrode, and the solvent is allowed to evaporate.

2.3 Electrochemical Experiments

Determinations were conducted at 20 [°C], atmospheric pressure and using a 30% w/w solution of potassium hydroxide (KOH 85% Biopack) as the electrolyte. This solution was prepared by determining the mass of potassium hydroxide needed and adjusting it to the volume with the necessary amount of distilled water. Once bottled, two drops of colloidal dispersion of the non-ionic surfactant Triton X-100 (Biopack) were added.

The electrochemical cell, where the electrodes were evaluated, comprised a cubic container, various pairs of rectified blocks, two guide brackets, two mobile locks (all constructed from crystal acrylic), and four steel screws, [38].

The cubic container has, right in its center, a slot that extends along its side walls and base. This slot allows the delineation of the cathodic and anodic compartments. It is where the material to be used as a separator is placed. The separator material employed is Zirfon®, which is a porous composite material that consists of a polysulfone matrix with embedded zirconium oxide in powder form, manufactured based on the film-casting technique, [39]. Each electrode is secured to a guide bracket using two small stainless-steel screws. The rectified blocks serve to establish the distance between the pair of electrodes. These are placed between the side wall of the cubic container and the guide brackets. Each set of rectified blocks has a length determined by the cubic container, but a different width that allows studying the behavior of the electrodes at various distances between them. Once the separator, electrolyte, pair of rectified blocks, and guide brackets with the electrodes have been placed inside the container, each piece is secured by the mobile locks. These pieces are crucial for maintaining the established position throughout the entire experiment. When the electrochemical cell was prepared, electrical connections were established with a Fullenergy System DC Power Supply HY3020 (30 V / 20 A, 600 W). Current measurements were taken at various potentials ranging from 0.0 to 2.7 V, with the applied voltage difference incremented by 0.1 V every 30 seconds. Each electrode gap, determined by the rectified blocks, was analyzed at least four times. Standard deviation and standard error were calculated. Given that the system's temperature increases after each experiment, to return to the initial working temperature, it was allowed to cool to room temperature.

3 Results and Discussion

For the decomposition of the water molecule to be successfully carried out, the energy required to overcome several barriers inherent to the electrochemical process must be provided. These obstacles encompass the electrical resistance within the circuit, the activation energies required for the hydrogen and oxygen evolution reactions at the electrode surfaces, the availability of electrode surfaces hindered by gas bubbles, and the resistance to ionic transfer within the electrolyte solution.

Electrical resistances can be determined using Ohm's law: R = V/I, where *I*, is the current flowing through the circuit when a voltage V, is applied. Alternatively, resistances can be calculated using the physical formula: R = L/(kA), where L represents the length of the conductor, k is the specific conductivity, and A is the cross-sectional area.

Related to the electrical resistance, different distances between electrodes were chosen to evaluate both types of geometries. Since the electrochemical cell establishes the distances using rectified blocks and the electrode's thickness, the values obtained are not the same in both experiments.

In Figure 2(a), are the polarization curves obtained by evaluating the flat stainless-steel electrodes at the following distances: 7.51; 6.10, and 4.59 [mm]. As the distances between electrodes get closer, the current density increases. It is important to keep in mind that current density is a parameter related to the number of products being formed, so a higher value implies greater production of hydrogen and oxygen. In this graphical representation (Figure 2(a)), it can also be observed that, although the reduction in distance from 7.51 [mm] to 6.10 [mm] and from 6.10 [mm] to 4.59 [mm] is very similar (on average 1.46 [mm]), in the latter pair mentioned, another phenomenon begins to appear, related to the formation and detachment of bubbles that increase resistance, and a comparable increase in current density is not observed as it is between 7.51 [mm] and 6.10 [mm].

In Figure 2(b), it can see the percentage increase in current density when comparing only the closest (4.59 [mm]) and farthest electrode distances (7.51 [mm]). As soon as the necessary potential for water decomposition is applied under these operating conditions, there is a very noticeable increase that later decreases until reaching a plateau at 2.3 [V] with a 40% enhancement.

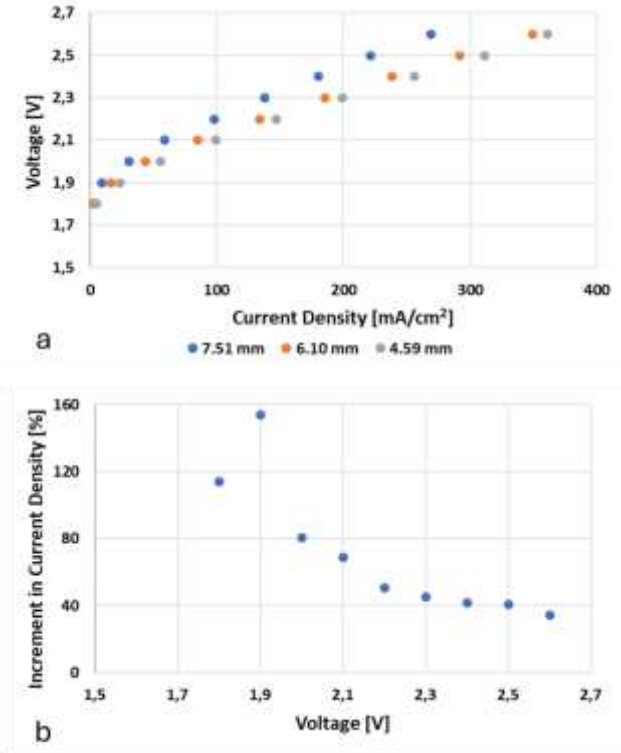

Fig. 2: Flat electrodes: a) polarization curves at 20°C and b) its percentage increase in current density

In Figure 3(a), are the results obtained for the pin-type geometry electrodes analyzed by the distances: 5.80; 3.53; 3.02, and 1.95 [mm], and the polarization curves acquired can be seen. The results are consistent with the previous ones; as the electrodes get closer, the current density rises, in the distances tested in this work. Figure 3(b), shows the percentage increase in current density for the closest (1.95 [mm]) and farthest (5.80 [mm]) distances between electrodes. After applying the minimum potential for water decomposition under these conditions, the percentage also increases rapidly and starts to gradually decrease from 2 [V] until apparently reaching a plateau at 2.5 [V]. This decrease can be attributed to the fact that with higher applied potential differences, bubbles fail to detach properly, which evens out the performance of the electrodes.

As the current density affects the amount of hydrogen and oxygen production; a higher current density leads to a faster rate of electrochemical reactions. However, the increased gas production rate causes rapid bubble formation, which raises the overpotential due to the additional resistance from the bubbles that partially cover the electrode surface until they detach.

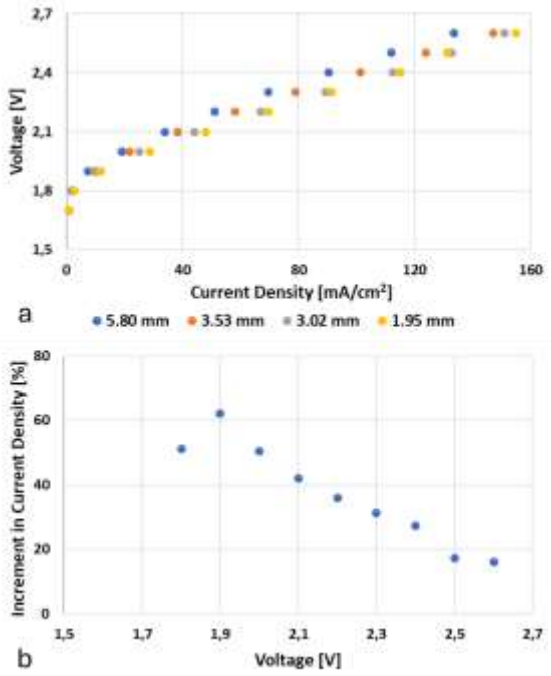

Fig. 3: Pin-type electrodes: a) polarization curves at 20°C and b) its percentage increase in current density

Table 1 presents the average values obtained from the standard deviations and the standard error for each of the distances evaluated. With the standard deviation, the aim is to show how dispersed the data from the four tests are about the mean. Since the presented values are small, it indicates that they are close to the average and that the results obtained from the conducted experiments are reproducible. For the standard error, the goal is to verify how much the sample mean might vary compared to the true population average. The presented values indicate that the results are consistent and that there is little variability in the central value of the different determinations made.

Table 1. Average of standard deviation and standard error for determination of "Flat" and ¨Pin-type¨ electrodes.

Electrodes	Distance [mm]	Standard Deviation	Standard Error
Flat	7.51	1.16	0.58
Flat	6.30	2.05	0.92
Flat	4.59	3.84	2.22
Pin-type	5.80	0,93	0.47
Pin-type	3.53	0.72	0.36
Pin-type	3.02	0.57	0.28
Pin-type	1.95	0.49	0.35

To compare the results obtained from both electrodes, distances between them that were as similar as possible were sought. Figure 4(a), exhibits the polarization curves for two distances of the pin-type electrodes and one for the flat electrodes. It is clear that the current density achieved by the flat electrodes is higher than that of the pin-type electrodes. Figure 4(b), presents that this increase on average is approximately 180 percent at a distance of 5.80 [mm] and 150 for the 3.53 [mm].

Since the only difference between determinations, besides the distances between electrodes, is the geometry on which the electrochemical reactions occur, the variation could be attributed to the behavior of bubbles on the surface.

During the water electrolysis process, hydrogen and oxygen bubbles form on the surface of the cathode and anode, respectively. However, these bubbles are only released when they reach a significant size. As mentioned at the beginning of this section, the presence of these bubbles, which partially cover the electrode surfaces until they reach the appropriate size, increases the overall electrical resistance of the system. This is because the bubbles reduce the contact area between the electrode surface and the electrolyte, hinder electron transfer, and consequently increase ohmic losses throughout the system. By obstructing the active area of the electrode, they decrease the system's efficiency. The addition of two drops of a colloidal dispersion of the non-ionic surfactant Triton X-100 aims to reduce the surface tension of the electrolyte used.

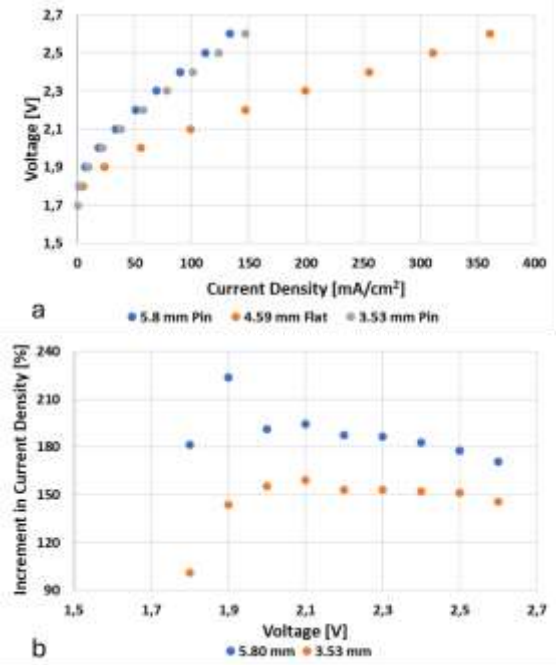

Fig. 4: Flat vs Pin-type electrodes: a) polarization curves at 20°, 5.80 [mm], and 3.53 [mm] for pin-type and 4.59 [mm] for flat and b) its percentage increase in current density

The electrical resistances in a water electrolysis system thus include mass transport phenomena, partial coverage of the electrodes and diaphragm by the generated bubbles, and the inherent resistance in the system's circuits, [40], [41]. Electrical resistance directly causes heat generation, resulting in the loss of electrical energy in the form of heat and this is the reason why to produce the same amount of product more energy is required. The heat released is the product of the applied voltage difference and the current density. Therefore, the heat released for these three systems will be discussed. At the same current density, it could be observed (Figure 5(a)) that the systems where the pin-type electrodes are evaluated, released more heat to generate an equal amount of hydrogen than the one, with flat electrodes. In Figure 5, the two graphical representations show the same results; however, Figure 5(b), displays the initial values to better appreciate this fact. For the case of the flat electrode, at a current density of 99,37 [mA/cm²], less heat is released compared to the pin-type electrode at 3.53 [mm] with a current density of 101,39 [mA/cm²] (208,68 and 243,33 [mW s/cm²] respectively). The same can be said for the same type of electrode at 5.80 [mm], as it releases a greater amount of heat (216,96 [mW s/cm²]) even at a lower current density (90,40 [mA/cm²]).

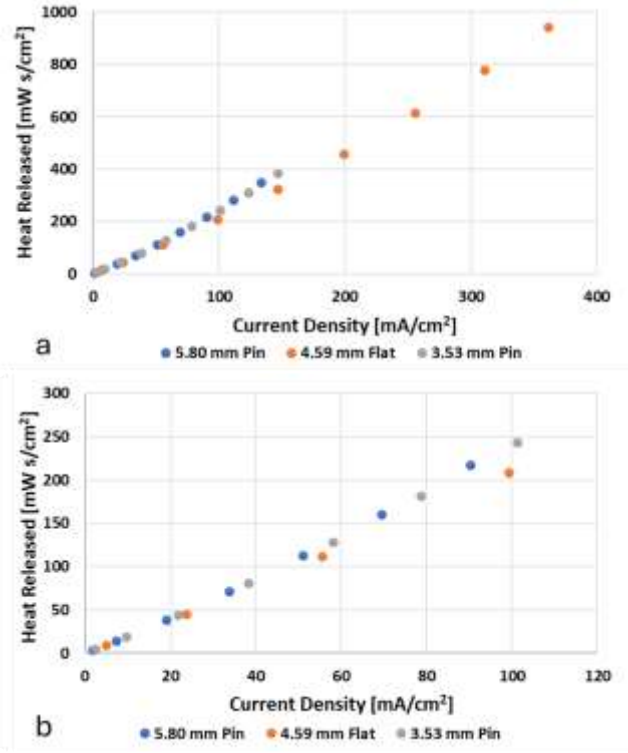

Fig. 5: Heat released vs current density from 0 to: a) 2.7 [V] and b) 2.3 [V]

The electrode with pin-type geometry affects the detachment of the generated bubbles. The straight walls of the pins seem to be the favorable spots for bubble accumulation, which, by remaining longer, prevent the electrode surface from being available for the electrochemical process. Another point that should be considered in future work is whether the recirculation of the electrolyte could improve this situation as well as the homogenization of the electrolyte solution concentration near the active area. Although this geometry results in an approximately 83% increase in the exposed surface area of the electrode, the results show a noticeable detriment in this specific process.

4 Conclusion

The behavior of two different electrode topologies has been evaluated: flat and pin-type. The pin type, despite having an active surface area 83 percent larger than the flat type, did not show a comparable increase in current density. This fact may be directly related to the bubbles generated on the electrode surface. The pins do not facilitate the rapid release of bubbles, which accumulate over long periods, rendering the surface ineffective. As a result, overpotentials and ohmic losses appear.

Concentration overvoltage arises from mass transport processes. Limited mass transport increases the concentration of products between the electrode and the electrolyte and consequently reduces the concentration of reagents. Ohmic losses are the result of the resistance of various cell components and the gas bubbles covering the electrode surface. To overcome the barriers, a higher voltage is required to obtain the same amount of product, and the energy losses result in a greater amount of heat released.

In electrochemical processes that involve bubble formation, geometries that increase the active area are required, as long as they also promote bubble formation and rapid detachment. In this case, using the material as it comes from the factory is the best option, since the horizontal channels and the pins generated by the intersections retain bubbles for a prolonged period and decrease the inherent efficiency of the material used.

Disclosure:
The manuscript is based on the oral presentation at the 2nd International Conference on Electrical Engineering and Computational Science.

Acknowledgement:
The authors of this manuscript thank the Argentinean Ministry of Defense and the Authorities of the Institute of Scientific and Technical Research for Defense (CITEDEF) for their financial support through the subsidy PIDDEF 04/2020.

References:

[1] M. Nachmany, S. Fankhauser, J. Davidová, N. Kingsmill, T. Landesman, H. Roppongi, P. Schleifer, J. Setzer, A. Sharman, C.S. Singleton, J. Sundaresan, T. Townshend. The 2015 global climate legislation study: a review of climate change legislation in 99 countries: summary for policy-makers. London, UK: Grantham Research Institute on Climate Change and the Environment, GLOBE International, 2015, [Online]. https://www.lse.ac.uk/granthaminstitute/wp-content/uploads/2015/05/Global_climate_legislation_study_20151.pdf (Accessed Date: October 30, 2024).

[2] O. Jianu, D. Pandya, M.A. Rosen, G. Naterer. Life cycle assessment for thermolysis and electrolysis integration in the copper-chlorine cycle of hydrogen production. *WSEAS Transactions on Environment and Development*, Vol. 12, 2016, pp. 261-267.

[3] H.M. Enshasy, Q.A. Al-Haija, A. Al-Amri, M. Al-Nashri, S. Al-Muhaisen, M. Al-Tarayrah. A comprehensive construction of hydrogen-hydrogen-oxygen (HHO) cell as renewable energy storage. *WSEAS Transactions on Systems*, Vol. 19, 2020, pp. 121-132. https://doi.org/10.37394/23202.2020.19.17.

[4] International Energy Agency. *CO_2 Emissions in 2023. A new record high, but is there light at the end of the tunnel?* France, IEA Publications, 2024, [Online]. https://www.iea.org/reports/co2-emissions-in-2023 (Accessed Date: October 30, 2024).

[5] T.-Z. Ang, M. Salem, M. Kamarol, H. Shekhar Das, M. Alhuyi Nazari, N. Prabaharan. A comprehensive study of renewable energy sources: Classifications, challenges and suggestions, *Energy Strategy Reviews*, Vol. 43, 2022, 100939. DOI: 10.1016/j.esr.2022.100939.

[6] G. Notton, M.-L. Nivet, C. Voyant, C. Paoli, C. Darras, F. Motte, A. Fouilloy. Intermittent and stochastic character of renewable energy sources: Consequences, cost of intermittence and benefit of forecasting, *Renewable and Sustainable Energy Reviews*, Vol. 87, 2018, pp. 96-105. DOI: 10.1016/j.rser.2018.02.007.

[7] F. Ramos, A. Pinheiro, R. Nascimento, W. de Araujo Silva, M. A. Mohamed, A. Annuk, M. H. N. Marinho. Development of Operation Strategy for Battery Energy Storage System into Hybrid AC Microgrids, *Sustainability*, Vol. 14, No. 21, 2022, 13765. DOI: 10.3390/su142113765.

[8] L. Wagner. *Overview of energy storage methods. Research report*. Mora Associates, 2007, [Online]. http://www.moraassociates.com/publications/0712%20Energy%20storage.pdf (Accessed Date: June 17, 2024).

[9] H.A. Kiehne. *Battery Technology Handbook*. Boca Raton: CRC Press; 2003, p. 542.

[10] M.S. Guney, Y. Tepe Y. Classification and assessment of energy storage systems, *Renewable and Sustainable Energy Reviews*, Vol. 75, 2017, pp.1187–1197. DOI: 10.1016/j.rser.2016.11.102.

[11] R. Kumar, D. Lee, Ü. Ağbulut, S. Kumar, S. Thapa, A. Thakur, R. D. Jilte, C. A. Saleel, S. Shaik. Different energy storage techniques: recent advancements, applications, limitations, and efficient utilization of sustainable energy, *Journal of Thermal Analysis and Calorimetry*, Vol. 149, 2024, pp. 1895–1933. DOI: 10.1007/s10973-023-12831-9.

[12] M. K. Khan, M. Raza, M. Shahbaz, U. Farooq, M. U. Akram. Recent advancement in energy storage technologies and their applications, *Journal of Energy Storage*, Vol. 92, 2024, 112112. DOI: 10.1016/j.est.2024.112112.

[13] H. Chen, T. N. Cong, W. Yang, C. Tan, Y. Li, Y. Ding. Progress in electrical energy storage system: A critical review, *Progress in Natural Science*, Vol. 19, No. 3, 2009, pp. 291-312. DOI: 10.1016/j.pnsc.2008.07.014.

[14] M. A. Vaziri Rad, A. Kasaeian, X. Niu, K. Zhang, O. Mahian. Excess electricity problem in off-grid hybrid renewable energy systems: A comprehensive review from challenges to prevalent solutions, *Renewable Energy*, Vol. 212, 2023, pp. 538-560. DOI: 10.1016/j.renene.2023.05.073.

[15] A. Zerrahn, W.-P. Schill, C. Kemfert. On the economics of electrical storage for variable renewable energy sources, *European Economic Review*, Vol. 108, 2018, pp. 259-279. DOI: 10.1016/j.euroecorev.2018.07.004.

[16] A. S. Mohd Razif, N. F. Ab Aziz, M. Z. A. Ab Kadir and K. Kamil. Accelerating energy transition through battery energy storage systems deployment: A review on current status, potential and challenges in Malaysia, *Energy Strategy Reviews*, Vol. 52, 2024, 101346. DOI: 10.1016/j.esr.2024.101346.

[17] S. Ould Amrouche, D. Rekioua, T. Rekioua, S. Bacha. Overview of energy storage in renewable energy systems, *International Journal of Hydrogen Energy,* Vol. 41, No. 45, 2016, pp. 20914-20927. DOI: 10.1016/j.ijhydene.2016.06.243.

[18] V. Mladenov, V. Chobanov, E. Zafeiropoulos, V. Vita. Characterisation and evaluation of flexibility of electrical power system, *2018 10th Electrical Engineering Faculty Conference (BuIEF 2018),* Sozopol, Bulgaria, 2018, pp. 1-6.

[19] T. Bowen, I. Chernyakhovskiy, P. Denholm. Grid-Scale Battery Storage Frequently Asked Questions. *National Renewable Energy Laboratory/TP-6A20-74426*, 2019, pp. 1-8, [Online]. https://www.nrel.gov/docs/fy19osti/74426.pdf (Accessed Date: October 30, 2024).

[20] M. J. Palys, P. Daoutidis. Power-to-X: A review and perspective, *Computers & Chemical Engineering.* Vol. 165, 2022, 107948. DOI: 10.1016/j.compchemeng.2022.107948.

[21] IRENA. *Innovation landscape for a renewable-powered future: Solutions to integrate variable renewables. Preview for policy makers.* Abu Dhabi: International Renewable Energy Agency, 2019, [Online]. https://www.irena.org/-/media/Files/IRENA/Agency/Publication/2019/Feb/IRENA_Innovation_Landscape_2019_report.pdf (Accessed Date: October 30, 2024).

[22] R. Daiyan, I. MacGill, R. Amal, Opportunities and Challenges for Renewable Power-to-X, *ACS Energy Letters*, Vol. 5, No. 12, 2020, pp. 3843–3847. DOI: 10.1021/acsenergylett.0c02249.

[23] B. Rego de Vasconcelos, J.-M. Lavoie, Recent Advances in Power-to-X Technology for the Production of Fuels and Chemicals, *Frontiers in Chemistry,* Vol. 7, 2019, 392. DOI: 10.3389/fchem.2019.00392.

[24] M. Sterner, M. Specht, Power-to-Gas and Power-to-X—The History and Results of Developing a New Storage Concept, *Energies*, Vol. 14, 2021, 6594. DOI: 10.3390/en14206594.

[25] A.R. Dahiru, A. Vuokila, M. Huuhtanen, Recent development in Power-to-X: Part I – A review on techno-economic analysis, *Journal of Energy Storage*, Vol. 56, 2022, 105861. DOI: 10.1016/j.est.2022.105861.

[26] M. Jentsch, T. Trosta, M. Sterner, Optimal Use of Power-to-Gas Energy Storage Systems in an 85% Renewable Energy Scenario, *Energy Procedia*, Vol. 46, 2014, pp. 254-261. DOI: 10.1016/j.egypro.2014.01.180.

[27] N. S. Muhammed, B. Haq, D. Al Shehri, A. Al-Ahmed, M. M. Rahman, E. Zaman. A review on underground hydrogen storage: Insight into geological sites, influencing factors and future outlook, *Energy Reports*, Vol. 8, 2022, pp. 461-499. DOI: 10.1016/j.egyr.2021.12.002.

[28] M. Reisert, A. Aphale, S. Prabhakar, Solid Oxide Electrochemical Systems: Material Degradation Processes and Novel Mitigation Approaches. *Materials,* Vol. 11, 2018, 2169. DOI: doi.org/10.3390/ma11112169.

[29] C.M. Kalamaras, A.M. Efstathiou, Hydrogen Production Technologies: Current State and Future Developments. *Hindawi. Conference Papers in Energy*, Vol. 2013, 2013, Article ID 690627. DOI: 10.1155/2013/690627.

[30] H. Strathmann. Electrochemical and Thermodynamic Fundamentals. Ion-Exchange Membrane Separation Processes, *Membrane Science and Technology*, Elsevier Science, Vol. 9, 2007, pp. 23-88.

[31] S. Shiva Kumar, H. Lim, An overview of water electrolysis technologies for green hydrogen production, *Energy Reports*, Vol. 8, 2022, pp. 13793-13813. DOI: 10.1016/j.egyr.2022.10.127.

[32] S. Shiva Kumar, V. Himabindu, Hydrogen production by PEM water electrolysis – A review, *Materials Science for Energy Technologies*, Vol. 2, 2019, pp. 442-454. DOI: /10.1016/j.mset.2019.03.002.

[33] C. Bettenhausan, Electrolyzers: The tools to turn hydrogen green. *C&EN Global Enterprise*, Vol. 101, No. 21, 2023, pp. 25-30, [Online]. https://cen.acs.org/materials/electronic-materials/Electrolyzers-tools-turn-hydrogen-green/101/i21 (Accessed Date: October 30, 2024).

[34] M. Nikologiannis, I. Mozakis, I. Iliadis, Y. Katsigiannis. Financial assessment of microgrid's independence using RES and hydrogen-based energy storage. *WSEAS Transactions on Power Systems*, Vol. 19,

2024, pp. 307-321. https://doi.org/10.37394/232016.2024.19.27.

[35] A. Y. Faid, S. Sunde, Anion Exchange Membrane Water Electrolysis from Catalyst Design to the Membrane Electrode Assembly, *Energy Technol*., Vol. 10, 2022, 2200506. DOI: 10.1002/ente.202200506

[36] A. W. Tricker, J. K. Lee, J. R. Shin, N. Danilovic, A. Z. Weber, X. Peng, Design and operating principles for high-performing anion exchange membrane water electrolyzers, *Journal of Power Sources*, Vol. 567, 2023, 232967. DOI: 10.1016/j.jpowsour.2023.232967.

[37] D. Hua, J. Huang, E. Fabbri, M. Rafique, B. Song, Development of Anion Exchange Membrane Water Electrolysis and the Associated Challenges: A Review. *ChemElectroChem*, Vol. 10, 2023, e202200999. DOI: 10.1002/celc.202200999.

[38] M.J. Lavorante, R. Diaz Bessone, S. Saiquita, R.M. Aiello, E.Al. Ramírez Martínez. Performance of an electrode topology for alkaline water electrolysis under specific operating conditions. *Design, Construction, Maintenance*, Vol. 2, 2022, pp. 98-107. DOI: 10.37394/232022.2022.2.15.

[39] H.I. Lee, D.T. Dung, J. Kim, J.H. Pak, S.K. Kim, H.S. Cho, W.C. Cho and C.H. Kim, The synthesis of a Zirfon-type porous separator with reduced gas crossover for alkaline electrolyzer, *International Journal of Energy Research*, Vol. 44, 2020, pp. 1875-1885. DOI: 10.1149/MA2019-02/37/1756.

[40] W. Li, H. Tian, L. Ma, Y. Wang, X. Liu, X. Gao. Low-temperature water electrolysis: fundamentals, progress, and new strategies, *Material Advances*, Vol. 3, 2022, 5598. DOI: 10.1039/D2MA00185C.

[41] K. Zeng, D. Zhang. Recent progress in alkaline water electrolysis for hydrogen production and applications, *Progress in Energy and Combustion Science*, Vol. 36, 2010, pp. 307–326. DOI: 10.1016/j.pecs.2009.11.002.

Contribution of Individual Authors to the Creation of a Scientific Article (Ghostwriting Policy)

- María José Lavorante has diagrammed the experiments, executed part of the determinations, analyzed the data obtained, constructed the graphical representations, and drafted the manuscript.
- Micaela Fragueiro Frias has conducted part of the experiments.
- Nelson Jesús Vichera Mola has conducted part of the experiments.
- Marcelo Bustos has built the geometry in the electrodes.

Sources of Funding for Research Presented in a Scientific Article or Scientific Article Itself

PIDDEF 04/2020 granted by the Argentinean Ministry of Defense and the Authorities of the Institute of Scientific and Technical Research for Defense.

Conflict of Interest

The authors have no conflicts of interest to declare.